Optimal fluids for adsorptive cooling and heating

Optimal fluids for adsorptive cooling and heating

Giulio Santori, Chiara Di Santis

Abstract

The search for optimal fluid/adsorbent working pairs in adsorption heat transformers is featured by trial and error method. In the last decades this approach has produced relevant progresses especially resulted in new advanced adsorption materials. On the refrigerant fluid side water, ammonia, methanol and ethanol still seem to be the only viable options. This work aims to explain the reason of that and the requirement that a refrigerant fluid must fulfil in order to be considered as promising for adsorptive cooling and heating. A thermodynamic framework is developed that merges the corresponding states principle with the characteristic curve of adsorption. Finally the framework is applied to assess the theoretical coefficient of performance of 258 fluids on 16 adsorption materials belonging to activated carbons, silica gels and zeolites, by avoiding in this way blind search strategy of the optimal working pair. Furthermore, the approach is used also to identify more generally the refrigerant thermodynamic properties for maximum performance. Fluid critical temperature is often the chief property enabling higher performance, although not always all the adsorption materials share the same sensitivity to the same thermodynamic properties.

1.Introduction

The recent progress in adsorption materials with extraordinary equilibrium properties has primed an increase of performance in thermally-driven adsorption technologies that can use heat at temperatures <373 K and convert it in a useful effect such as cold, separation or compression [1-8]. Few solutions exist capable of usefully transforming such a low quality heat that is therefore often wasted. Adsorptive heat pumps and chillers are among these solutions. To date, research in this area has been mainly focused on material [9, 10], heat and mass transfer enhancement [11-13], process [14-18] and component optimization [19, 20]. Conversely, research and development of bespoke refrigerant fluids has been minimal, resulting in the identification of water, ammonia, methanol and ethanol as viable fluids. The few analyses on this subject aimed to develop an adsorption thermodynamic cycle independent of the properties of fluids [21-23]. All these attempts ended up with the need for specification of a working pair [21] or with uncertainties in the conclusions [23]. In [21] was concluded that latent heat of the fluid should have a value >1000 kJ kg^{-1} and any other increase of this value does not provide a significant increase of the coefficient of performance (COP). This conclusion was derived by fixing working capacity at 0.1 kg$_{fluid}$ kg$^{-1}_{ads}$. Being the adsorption working capacity dependent on the fluid/adsorbent working pair, this is a strong assumption which makes the conclusions less general. The same issue is present in analyses elsewhere [23, 24], where the difficulty to isolate the single effect respectively of fluid and material on the COP has been highlighted.

Therefore, every conclusion is valid only for the specific working pair at the specific set of operating temperatures and conditions. The attempts for extending the results to different fluids and materials have provided no clear direction on the features that a fluid must have for optimal COP.

In order to overcome this issue, the urgency of a large database of isotherms which can enable the direct search of optimal working pair has been stated elsewhere [25-27] and some small adsorption databases are already available [28-30] which, however, still require large improvement and a constant screening and integration of the huge amount of new experimental data measured every year.

This work addresses directly the issues of the blind working pair search. The approach developed here merges the corresponding states principle [31] and the characteristic curve of adsorption [32], resulting in a general formulation requiring experimental data from only one working pair. From this approach, the identification of fluid specifications enabling maximum COP is also derived.

2.Thermodynamics of adsorption heat transformers

Fig. 1 is exemplar of a thermodynamic cycle for adsorption refrigeration in the Claperyron diagram. The set of temperatures typical of air conditioning are regeneration temperature (T_{reg}) of 363 K, condensing temperature (T_{cond}) of 303 K and evaporation temperature (T_{ev}) of 283 K. This temperature set will be used

throughout this study. An adsorption heat transformer works at T_{cond} and T_{ev} saturation pressures (P_{sat}). The adsorption isosteres are used to locate the cycle in the Clapeyron diagram.
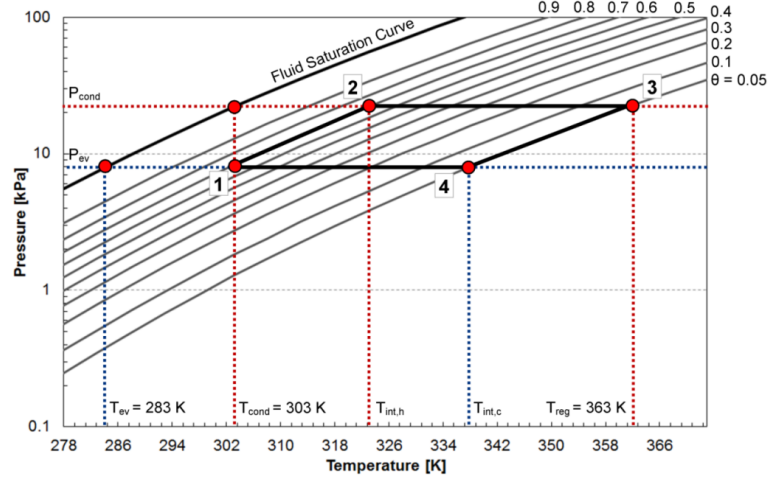

Figure 1: General thermodynamic cycle for adsorption refrigeration

The cycle is composed by 4 thermodynamic transformations:

1) States 1-2: isosteric heating. The adsorption bed is heated (Q_{ph}) at constant concentration until it reaches the condensation pressure P_{cond}.
2) States 2-3: desorption. An amount of heat Q_{des} is provided to regenerate the adsorption bed.
3) States 3-4: isosteric cooling. The adsorption bed is cooled until reaches the evaporation pressure P_{ev}.
4) States 4-1: adsorption. The adsorption bed is continuously cooled while it increases its concentration. The difference between the maximal and minimal isostere is the amount of fluid evaporated (cooling effect).

The described cycle is in its nature intermittent since it generates cooling only in transformation 4-1. The cooling effect can be made continuous by using at least two adsorption beds that work alternatively. One bed will be in 2-3 while a second in 4-1 transformation. A more extensive description of the cycle can be found elsewhere [33]. Neglecting the parasitic energy required for heating of non-active masses and the pressure drops in the system, COP is defined as:

$$COP = \frac{Q_{ev}}{Q_{des}+Q_{ph}} \tag{1}$$

where

$$Q_{ph} = q_1 \bar{c}_{p,refr}(T_{int,h} - T_{cond}) + \bar{c}_{p,ads}(T_{int,h} - T_{cond}) \tag{2}$$

$$Q_{des} = \bar{c}_{p,ads}(T_{reg} - T_{int,h}) + \frac{(q_2-q_3)}{2}\bar{c}_{p,refr}(T_{reg} - T_{int,h}) + \int_{q_2}^{q_3} \Delta h_{ads} dq \tag{3}$$

$$Q_{ev} = (q_1 - q_4)[L|_{T_{ev}} - \bar{c}_{p,refr}(T_{cond} - T_{ev})] \tag{4}$$

for brevity the meaning of the subscripts is reported in the nomenclature section. By grouping the first term in eq. (2) with the second of eq. (3), COP can be also reformulated by using dimensionless terms as indicated in [33], resulting in the following expression:

$$COP = \frac{1-K_{refr}}{1+K_{1,ads/refr}+K_{2,ads/refr}} \tag{5}$$

where

$$K_{refr} = \frac{\bar{c}_{p,refr}}{L|_{T_{ev}}}(T_{cond} - T_{ev}) \tag{6}$$

$$K_{1,ads/refr} = \frac{\int_{q_2}^{q_3} \Delta h_{ads} dq - L|_{T_{ev}}(q_2 - q_3)}{L|_{T_{ev}}(q_2 - q_3)} \tag{7}$$

$$K_{2,ads/refr} = \frac{\bar{c}_{p,ads}}{L|_{T_{ev}}}(T_{reg} - T_{cond}) \tag{8}$$

A number of thermodynamic properties such as the latent heat (L) and heat capacities of fluid and material ($c_{p,ads}$ and $c_{p,refr}$) along with the adsorption isotherms are needed to calculate the COP. These relations require a number of thermophysical and thermodynamic fluid-specific parameters. A corresponding states principle-based thermodynamic analysis can provide a formulation which reduces all the thermodynamic properties only to critical temperature (T_{cr}), critical pressure (P_{cr}), critical density (ρ_{cr}), acentric factor (ω) and ideal gas

molar specific heat capacity at T_{cr} ($c_{p0,cr}$). Coupling this approach with the characteristic curve of adsorption theory [32], a general framework for the calculation of COP is obtained which requires only the above mentioned properties of the fluid and the measurement of one reference set of adsorption isotherms.

3. Generalization of fluid thermodynamics with corresponding states principle

In its simplest form, the corresponding-states principle [31] provides a correlation where each thermodynamic variable can be written as a function of T_{cr} and P_{cr} and ω. The corresponding state principle competes with a number of equations of states such as Soave-Redlich-Kwong [34], Peng-Robinson [35] and many others which, in the simplest cases, also have three substance-specific parameters. Here the corresponding state principle has been chosen since the fluids of interest in adsorption are often polar fluids [36, 37], therefore resulting in the failure of afore mentioned equation of states. Table 1 collects the corresponding states correlations used in the present investigation for the calculation of the thermophysical and thermodynamic properties of the fluids, such as saturation pressure (P_{sat}), molar latent heat (L), molar saturated liquid density (ρ_{sat}) and molar specific heat capacity (c_p). Details on the actual correlations can be found in support material S1.

Table 1: thermodynamic and thermophysical correlations used in the calculation of COP. Detailed correlations are reported in support material S1.

Correlation		AAD*	Ref
$L = f_1(T, T_{cr}, \omega)$	(9)	<5%	[38]
$P_{sat} = f_2(T, T_{cr}, P_{cr}, \omega)$	(10)	<5%	[38]
$\rho_{sat} = f_3(T, T_{cr}, \rho_{cr}, \omega)$	(11)	<9%	[39]
$c_{p,refr} = f_4(T, P, T_{cr}, P_{cr}, \omega, \rho_{cr}, c_{p0,cr})$	(12)	<8%	[40, 41]
*AAD = average absolute deviation			

Eq. (12) is based on a generalization of the Lee-Kesler corresponding-states equation of state [42] extended to fluids consisting of polar and larger non-polar molecules. The application of this equation of state has been limited to the calculation of the molar specific heat capacity because it lacks of precision when used for P_{sat}, L and ρ_{sat} compared to the other models used. The set of equations in Table 1 completes the description of the fluid, which in this way results identified only by a vector of fluid-specific entries ($T_{cr}, P_{cr}, \rho_{cr}, \omega, c_{p0,cr}$). A database of 258 fluids has been used in this work (support material S2), with values extracted from the Dortmund Data Bank [43].

4. Extension of the adsorption isotherm to all fluids: characteristic curve of adsorption

Each fluid/adsorbent working pair has its own adsorption equilibrium, described by specific adsorption isotherms. However, as observed in a number of cases [44-46], many adsorption materials exhibit a characteristic curve which can describe the relative adsorption (q/q_s) of fluids having similar thermodynamic properties. In an attempt of extending the corresponding state principle to adsorption, it has been demonstrated in [32] that for isotherms that can be reduced to the form *(ln(P/Psat) = J(T) X ψ(ϑ))*, where one temperature dependent term and one composition dependent term can be distinguished, the characteristic curve is defined by the following dimensionless group:

$$C(\theta) = \frac{q_s \, RT \, ln(P/P_{sat})}{\Delta G_{imm}} \tag{13}$$

where *C(ϑ)* is a universal dimensionless function of $\vartheta = q/q_s$ (fractional filling of pores or ratio between actual adsorbed amount and adsorbed amount at saturation). Parameters are the saturation capacity (q_s) and the immersion free energy of the solid in bulk liquid adsorbate (ΔG_{imm}). For an ideal gas, ΔG_{imm} corresponds to:

$$\Delta G_{imm} = RT \int_0^{q_s} ln(P/P_{sat}) \, dq \tag{14}$$

A test of validity of the characteristic curve approach applied to adsorption of benzene, cyclohexane, n-heptane and 1,2-dichloroethane on Davison PA-400 silica gel resulted in experimental equilibrium data remarkably collapsing on the *C(ϑ)* function [32]. Therefore, *C(ϑ)* is theoretically a general curve, which can be derived by using adsorption isotherms measured for only one reference fluid. The adsorbed amount of fluid different from the reference one can be theoretically calculated from *C(ϑ)*. The precision of *C(ϑ)* in the description of the actual adsorption equilibrium for fluids different from the reference one (the only one having actually measured data) depends on the similarity of the corresponding states thermodynamic parameters (i.e. T_{cr} and P_{cr}) with the reference fluid. The error in using *C(ϑ)* instead of a really measured

adsorption isotherm increases when the difference between the critical parameters of reference and non-reference fluid is high. The characteristic curve approach provides a value for ϑ but in order to retrieve q_s the application of Bachmann, Anderson and Gurvitsch's rule [47-50] is eventually required:

$$V_p = q_s/\rho_{sat} = constant \qquad (15)$$

Where $(1/\rho_{sat})$ is the molar volume of the saturated liquid and V_p is the total pore volume of the adsorption material. It is well known that the density of the adsorbed phase is not the density of the saturated liquid as it is in bulk phase vapour-liquid equilibrium [51-53]. However, the correct density of the adsorbed phase can be assessed with more advanced investigations not completely experimentally proved yet, requiring more complex approaches that cannot be reduced to the corresponding states thermodynamic parameters [53]. This work conserves the assumption that the adsorbed fluid is a saturated liquid as it has been assumed for decades to derive an expression of the Dubinin isotherm based on moles (or mass) instead of volume [54]. Dubinin-Astakhov (DA) isotherm is written according to the following expressions:

$$q_{DA} = q_s e^{-\left[\frac{RT}{E}ln\left(\frac{P_{sat}}{P}\right)\right]^t} \qquad (16)$$

Application of eq. (16) to eq. (14) leads to the following form of ΔG_{imm}:

$$\Delta G_{imm} = -q_s\, E\, Gamma\left[1+\frac{1}{t}\right] \qquad (17)$$

Where Gamma is the Gamma function. Therefore the characteristic curves for the DA isotherm result in:

$$C(P,T) = -\frac{RT\, ln(P/P_{sat})}{E\, Gamma\left[1+\frac{1}{t}\right]} \qquad (18)$$

Substitution of eq. (16) in eq. (18) provides a second expression for the characteristic curve which is only function of ϑ:

$$C(\vartheta) = \frac{\sqrt[t]{-ln(\vartheta)}}{Gamma\left[1+\frac{1}{t}\right]} \qquad (19)$$

5. Calculation of COP

Using the characteristic curve approach, COP has been calculated for 16 adsorption materials (Table 2) belonging to activated carbons, silica gels and zeolites on the 258 fluids listed in support material S2. The flowchart in Table 3 details the whole list of steps leading to the final COP value.

Table 2: Properties and isotherm parameters of the adsorption materials used in the present work.

Material[1]	Material Name	V_p	$C_{p,ads}$	Isotherm	Refrigerant	q_s	E	t	COP[3] (precise)	COP[4] (approx.)	Ref
		cm^3 kg^{-1}	kJ kg^{-1} K^{-1}			mol kg^{-1}	kJ mol^{-1}				
AC	A20	1028	0.90	DA	Ammonia	45.91	3.16	0.8	0.52	0.64	[55]
AC	A20	1028	0.90	DA	R-134a	27.26	7.72	1.4	0.35	0.42	[56]
AC	A20	1028	0.90	DA	Ethanol	17.30	6.35	2.0	0.63	0.72	[57]
AC	A20	1028	0.90	DA	R-134a	28.00	7.14	1.5	0.37	0.42	[58]
AC	A15	765	0.90	DA	Ethanol	12.37	8.05	2.0	0.55	0.69	[59]
AC	FR20	750	0.84	DA	Ethanol	12.72	13.50	2.0	0.41	0.63	[59]
AC	MaxsorbIII	1700	0.93	DA	Ethanol	26.05	5.54	1.8	0.66	0.75	[60]
AC	MaxsorbIII	1700	0.93	DA	Methanol	26.92	4.15	2.0	0.70	0.79	[61]
AC	MaxsorbIII	1700	0.93	DA	R-134a	42.22	8.70	1.2	0.38	0.46	[62]
AC	MaxsorbIII	1700	0.93	DA	n-Butane	13.76	17.44	1.1	0.19	0.38	[63]
AC	MaxsorbIII	1700	0.93	DA	R-134a	21.76	7.33	1.3	0.34	0.47	[58]
AC	MaxsorbIII	1700	0.93	DA	Propane	20.41	8.58	1.2	0.18	0.40	[58]
AC	SRD-1352/3	650	1.09	DA	Ammonia	33.42	4.40	1.1	0.48	0.60	[55]
AC	SRD-1352/3	650	1.09	DA	R-134a	20.10	9.73	1.8	0.23	0.31	[64]
AC	SRD-1352/3	650	1.09	DA	Ethanol	13.91	8.78	1.5	0.51	0.63	[59]
AC	AP4-60	470	0.77	DA	Ethanol	7.63	10.60	2.0	0.43	0.62	[59]
AC	ATO	640	0.98	DA	Ethanol	10.35	11.20	1.7	0.43	0.62	[59]
AC	COC-L1200	490	0.90	DA	Ethanol	7.46	13.30	2.0	0.34	0.57	[59]
AC	BPL	500	1.05	DA	Chloroethane	7.11	13.10	2.0	0.13	0.27	[65]
AC	207EA	464	0.93	DA	Methanol	10.30	6.57	1.7	0.54	0.68	[66]
AC	WS480	663	0.93	DA	Methanol	15.29	4.78	1.7	0.62	0.73	[66]
SG	Si/LiBr	650	0.82	DA	Ethanol	11.54	6.90	1.8	0.57	0.69	[59]
SG	Grace narrow pore	400	0.92	DA	Propane	4.68	5.05	1.2	0.14	0.25	[67]
SG	Grace narrow pore	400	0.92	DA	Propylene	4.93	7.09	1.3	0.12	N/A	[67]
SG	Grace wide pore	580	0.92	DA	Propane	2.05	4.67	1.2	0.08	0.30	[67]
SG	Grace wide Pore	580	0.92	DA	Propylene	2.65	4.78	1.0	0.08	N/A	[67]
ZEO	AQSOA-Z02[2]	277	0.75	DA	Water	17.21	7.00	3.0	0.72	0.80	[68, 69]
ZEO	ETS-10	119.5	0.80	DA	Water	7.16	20.28	2.0	0.26	0.50	[70]

Note:
[1] AC = Activated Carbon; SG = Silica Gel; ZEO = Zeolite;
[2] AQSOA-Z02/water equilibrium is described here by DA isotherm although this isotherm does not represent precisely the equilibrium. However, the present investigation is limited to DA isotherm. Isotherms different from DA would result in different expression of the characteristic curve outside the focus of the present study.
[3] COP is calculated by using precise thermodynamic properties and the DA isotherm parameters of the specific working pair.
[4] COP is calculated by using corresponding states approach and characteristic curve as described.

Table 3: List of steps for COP calculation with corresponding states and characteristic curve approach.

Step 1	Assignment: $(T_{cond}, T_{ev}, T_{reg})$ and calculation of (P_{cond}, P_{ev}) from $P_{sat}(T, T_{cr}, P_{cr}, \omega)$
Step 2	Θ_{MAX} and Θ_{min} are calculated from by equating: $$\sqrt[t]{-ln(\theta_{min})} = -\frac{RT_{reg}}{E} ln\left(P_{sat,cond}/P_{sat,reg}\right)$$ $$\sqrt[t]{-ln(\theta_{MAX})} = -\frac{RT_{cond}}{E} ln\left(P_{sat,ev}/P_{sat,cond}\right)$$
Step 3	The amount adsorbed in each state of the thermodynamic cycle is calculated by Bachmann, Anderson and Gurvitsch's rule : $q = \theta V_p \rho_{sat}(T, T_{cr}, \rho_{cr}, \omega)$
Step 4	$T_{int,h}$ and $T_{int,c}$ are calculated by equating: $T_{cond} ln\left(P_{sat,ev}/P_{sat,cond}\right) = T_{int,h} ln\left(P_{sat,cond}/P_{sat,int,h}\right)$ $T_{reg} ln\left(P_{sat,cond}/P_{sat,reg}\right) = T_{int,c} ln\left(P_{sat,ev}/P_{sat,int,c}\right)$
Step 5	All the remaining thermodynamic properties are calculated using: $L = f_1(T, T_{cr}, \omega)$ $c_{p,refr} = f_4(T, P, T_{cr}, P_{cr}, \omega, \rho_{cr}, c_{p0,cr})$
Step 6	Heat of adsorption is according to: $$\int_{q_{low}=\theta_{min}V_p\rho_{sat}}^{q_{high}=\theta_{MAX}V_p\rho_{sat}} \Delta h_{ads} dq \sim \int_{\theta_{min}}^{\theta_{MAX}} V_p \rho_{sat} \left[E\left(ln\left(\frac{1}{\theta}\right)\right)^{1/t} + L + \left(\frac{d}{dT}\left(\frac{1}{\rho_{sat}}\right)\right)\frac{E\rho_{sat}T}{t}\left(ln\left(\frac{1}{\theta}\right)\right)^{(1-t)/t} \right] d\theta$$ where $L = f_1(T, T_{cr}, \omega)$ $\rho_{sat} = f_3(T, T_{cr}, \rho_{cr}, \omega)$
Step 7	All the values are available for COP calculation

6. Influence of the material properties on the characteristic curve

The exponent t is the only equilibrium parameter taking part to eq. (19). Fig. 2 shows that for values <2.5, the t exponent has significant influence on the shape of the characteristic curve, whilst for values >2.5 the curve changes for only a small extent. Therefore, all fluid having same t will lay on the same curve and fluids having high values of t (>2.5) will share similar characteristic curve.
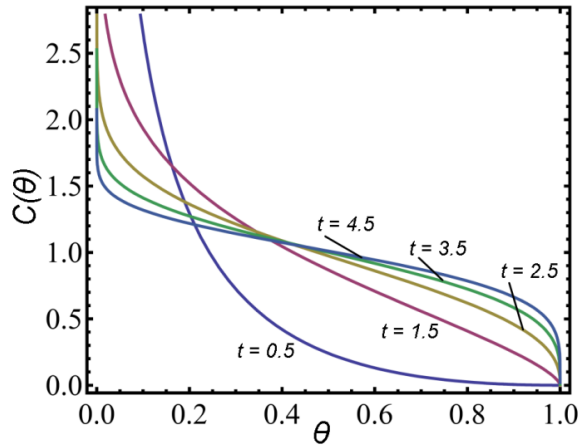

Figure 2: Characteristic curve of adsorption at various values of Dubinin-Astakhov isotherm exponent t

A comparison of the curves calculated for ethanol, methanol, n-butane and propane on MaxsorbIII is provided in Fig. 3 which shows very small mismatches respectively for ethanol/methanol and n-butane/propane. The experimental error in the isotherm parameters can impact consistently in these mismatches sometimes even more than the fluid properties difference. This is shown by Fig. 4, where a comparison of the different isotherms parameters obtained in two different laboratories [58, 62] for the same working pair MaxsorbIII/R-134a is reported.
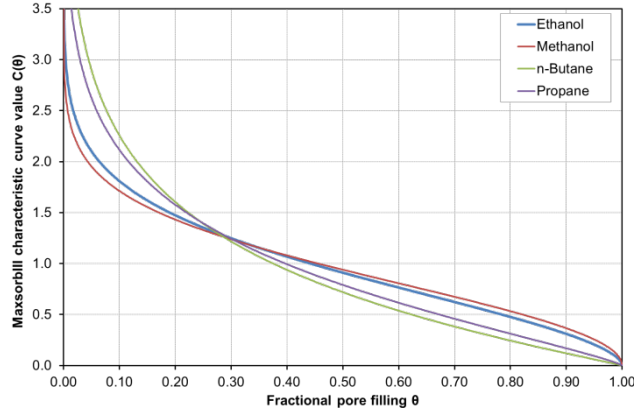
Figure 3: Characteristic curves for Ethanol, Methanol, n-Butane and Propane on MaxsorbIII
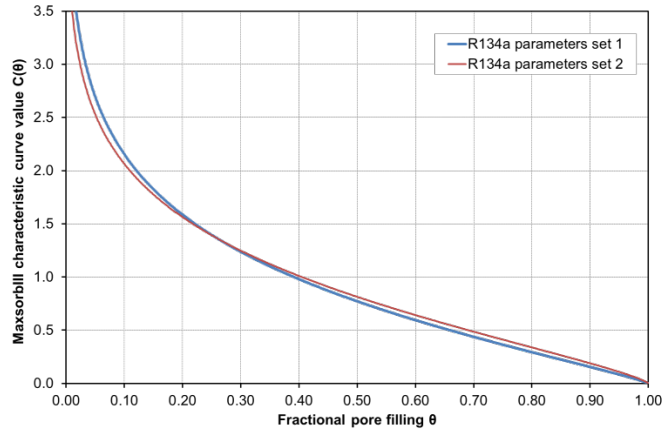

Figure 4: Characteristic curves of R134a on MaxsorbIII from two different laboratories [58, 62]. Set 1 is from [62], set 2 is from [58].

7.Influence of the fluid properties on the working capacity

Following up with the approach developed in [22], eq. (19) provides a good basis to locate directly on the characteristic curve the working states of the adsorption thermodynamic cycle. The important states for the quantitation of cycle performance are those related to the working capacity $\Delta\vartheta=(\vartheta_{MAX}-\vartheta_{min})$ where ϑ_{MAX} is the rich isostere and ϑ_{min} is the lean isostere which are identified on the characteristic curve by the following two values:

$$C_{lean}(P,T) = C_{lean}(\theta_{min}) = -\frac{RT_{reg}\,ln\left(P_{sat,cond}/P_{sat,reg}\right)}{E\,Gamma\left[1+\frac{1}{t}\right]} \tag{20}$$

$$C_{rich}(P,T) = C_{rich}(\theta_{MAX}) = -\frac{RT_{cond}\,ln\left(P_{sat,ev}/P_{sat,cond}\right)}{E\,Gamma\left[1+\frac{1}{t}\right]} \tag{21}$$

where $P_{sat,cond/ev/reg}$ are respectively the saturation pressures at T_{cond}, T_{ev} and T_{reg}. Saturation pressure can be expressed by eq. (10), ending up with a formulation which is dependent on the thermodynamic properties (T_{cr}, ω) of the fluid. The sensitivity of the working capacity to (T_{cr}, ω) is analysed in Fig. 5a and 5b. Fluids at higher T_{cr} and ω benefit of larger working capacities. Interestingly, the characteristic energy E which is one of the parameters of the DA isotherm, has an effect on the working capacity which is similar and inverse to (T_{cr}, ω). Fig. 5c shows that lower values for E promotes larger working capacities. In this formulation, the characteristic curve is independent from the parameter E.
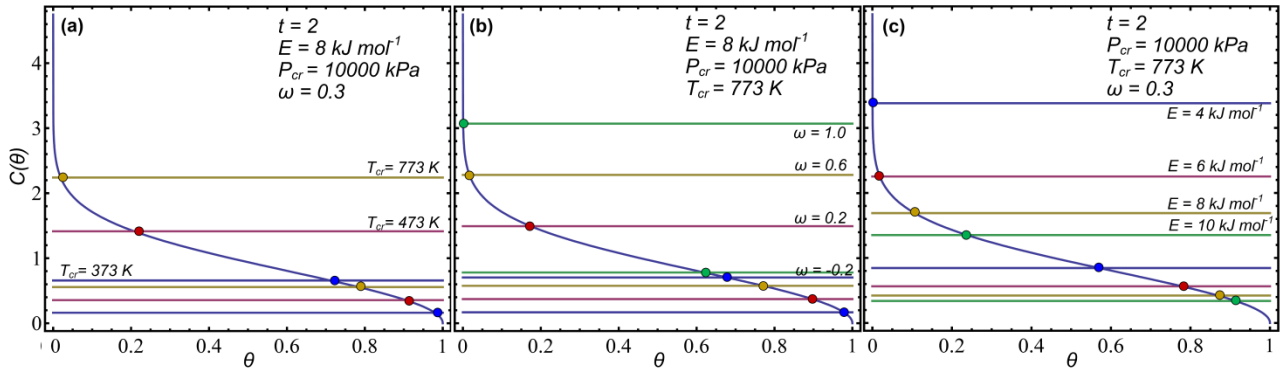
Figure 5: Influence of the fluid properties on the working capacity: (a) influence of the fluid critical temperature; (b) influence of the acentric factor; (c) influence of characteristic energy E for Dubinin-Astakhov isotherm.

8. Assumptions and limitations of the approach

The presented approach is valid within the following assumptions that include those of the corresponding states and characteristic curve theories:

- Mass of the heat exchangers is neglected;
- Vapour and adsorbed phases are ideal: all the expressions can be written as functions of pressure instead of fugacity and ΔG_{imm} can be reduced to eq. (18) [71];
- Adsorption equilibrium is best described by DA isotherm;
- The characteristic energy of adsorption E is the same for all fluids (used in step 2 calculation of Table 3);
- The fluid is adsorbed as a saturated liquid (Bachmann, Anderson and Gurvitsch's rule, eq. (15)) over the whole range of concentrations.

The present analysis has intrinsic errors. Errors are introduced by the characteristic curve approach which quantitatively represents actual adsorption isotherms only within a limited range of variation of the DA isotherm exponent t. Other approximations are introduced by the application of the corresponding states principle for the calculation of the fluid thermophysical and thermodynamic properties and by the combination of eq. (11) and eq. (15). Errors in the pore volume which is an information reported with low accuracy in the many references, and saturated liquid adsorbed fluid are the two weak assumptions of the present approach. Moreover, errors in saturated liquid affect not only directly the value of the working capacity but also the integration intervals of the enthalpy of adsorption. A check on the COPs, aimed to quantify the maximal errors is reported in Table 2 showing that the average error of the present approach is 28%. Therefore the present approach can identify relative but not absolute figures of merit.

9. Influence of the fluid properties on the dimensionless COP parameters

The dimensionless form of COP in eq. (5) allows the separate investigation of the three factors (K_{ref}, $K_{1,ads/ref}$, $K_{2,ads/ref}$) which have to be minimized for optimal COP. K_{ref} factor is function only of fluid properties and this is the reason of the overlap of many of the data in Fig. 6. From Fig. 6, minimal values of K_{ref} are at high critical temperature and critical pressure, with a decreasing rate smaller at $P_{cr} > 6500$ kPa.
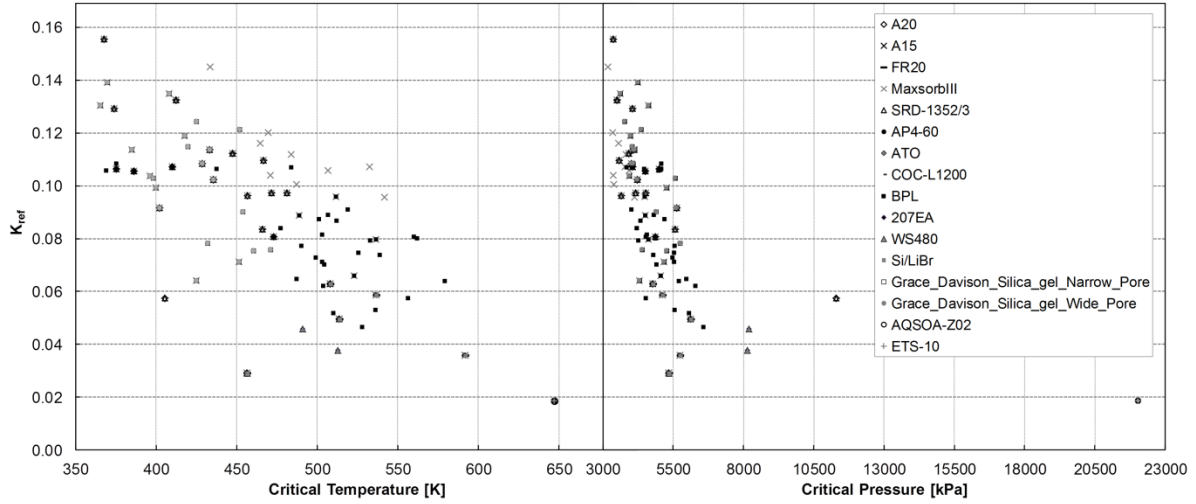
Figure 6: Dependence of K_{ref} on adsorbate critical temperature and critical pressure

$K_{1,ads/ref}$ factor is the ratio between heat of adsorption and latent heat of the fluid. As shown in Fig. 7, the value of this factor has a region of minima centred around T_{cr} = 400 K. Interestingly this region of critical temperatures includes Ammonia (T_{cr} = 405.65 K). The adsorption material governs the non-linearity of the correlation between $K_{1,ads/ref}$ and T_{cr}. Depending on the material, $K_{1,ads/ref}$ can be more or less strongly non-linearly correlated to T_{cr}.
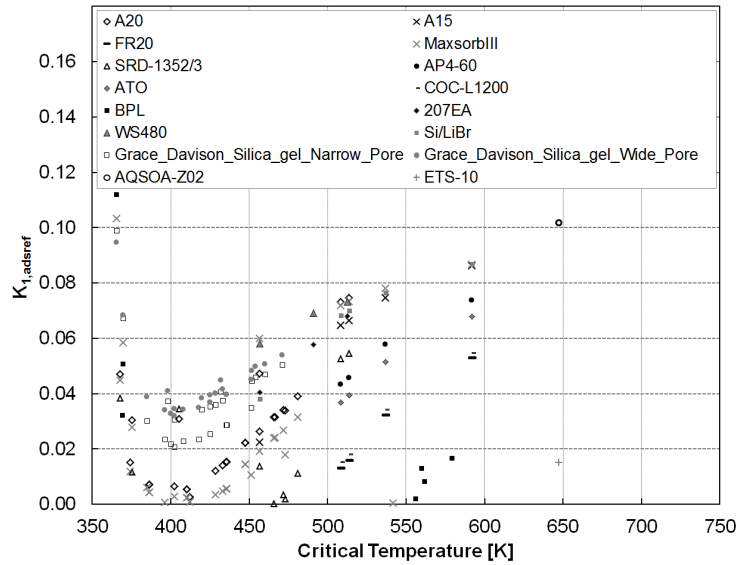

Figure 7: Variation of $K_{1,ads/ref}$ with adsorbate critical temperature

This study keeps the specific heat capacity value of the adsorption material constant across all the operational range of temperatures. This makes $K_{2,ads/ref}$ only a function of latent heat, which is here calculated according to eq. (9). So, its dependence is mostly on T_{cr} and P_{cr}, given that ω is defined on P_{cr}. Fig. 8 shows that, similarly to K_{ref}, $K_{2,ads/ref}$ can be minimized by using fluids at high T_{cr} and P_{cr} and fluids having P_{cr}>6500 usually have also low values of $K_{2,ads/ref}$. Nevertheless, there is a region of T_{cr} where $K_{2,ads/ref}$ is maximal. This region moves from material to material depending on the specific heat capacity of the material itself.
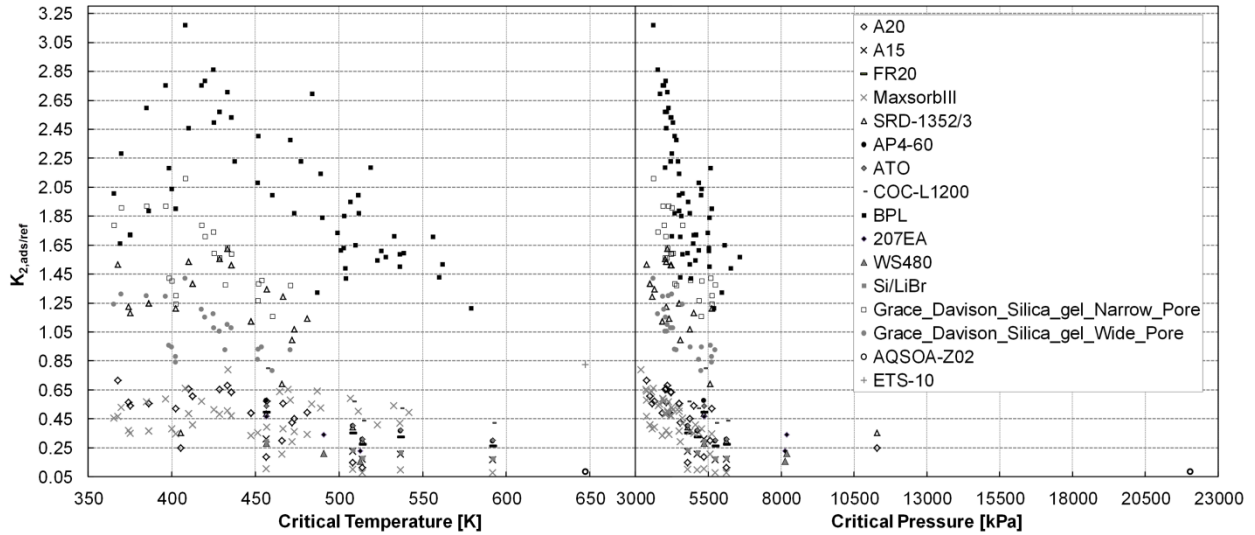
Figure 8: Dependence of $K_{2,ads/ref}$ on adsorbate critical temperature and critical pressure

10. Sensitivity of the COP to the fluid properties

The described approach cannot be applied for each adsorption material of Table 2 to the whole list of fluids because the reference characteristic curve is obtained only on one specific fluid. Therefore, as a criterion of similarity among fluids, only a neighbourhood centred in the values of the thermodynamic parameters of the reference fluid can still be considered reliable. Fluids falling in this neighbourhood are assumed adsorbing on the same characteristic curve of the reference fluid. Fig. 9 and 10 show the COP variation respectively with T_{cr} and ρ_{cr} when this neighbourhood is assumed in a ±30% region of the reference fluid properties. For all materials, fluids with higher T_{cr} and ρ_{cr} produce higher COP, but whilst COP and T_{cr} are fairly linearly correlated throughout the screened range, ρ_{cr} has a strong effect on COP only below 8000 mol m^{-3} and unevenly on all the adsorption materials. According to eq. (15), ρ_{cr} affects directly the adsorption saturation value q_s, so it is trivial that fluids with higher ρ_{cr} are beneficial for the COP.
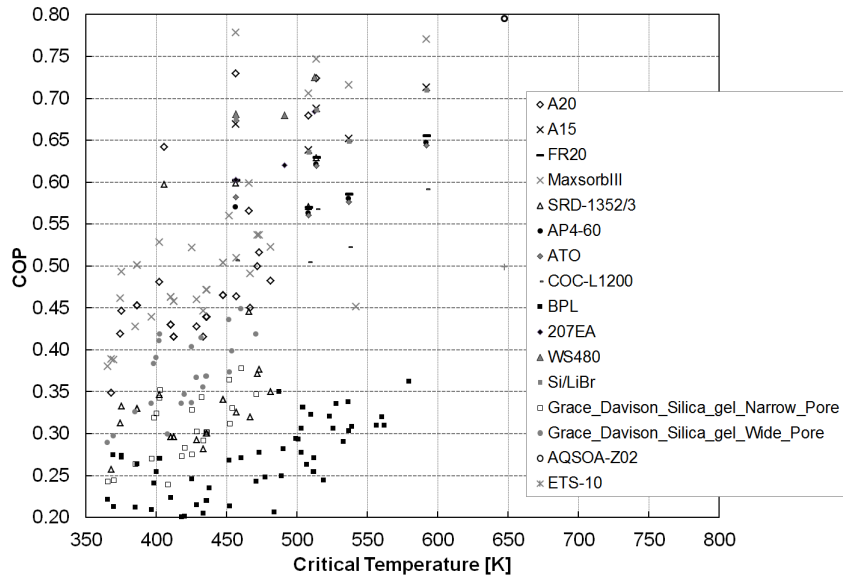

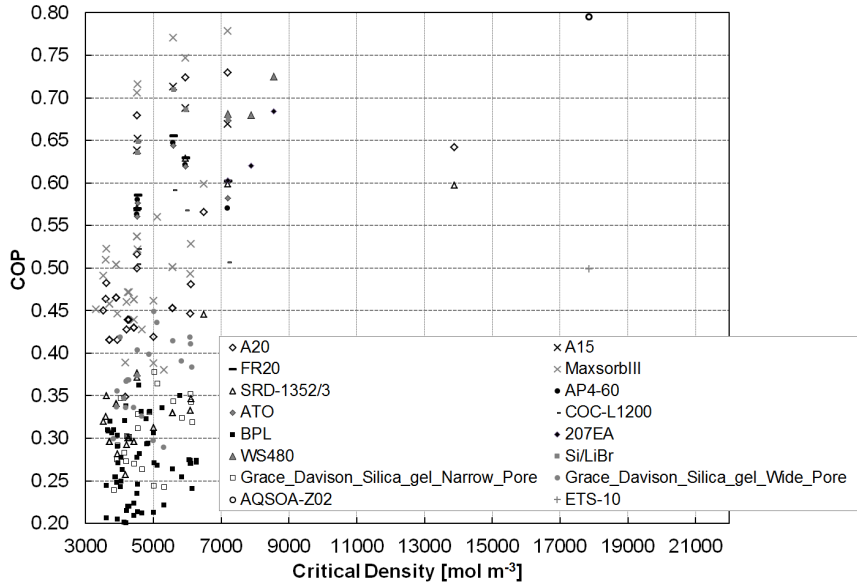Figure 9: Variation of the COP with the adsorbate critical temperature

Figure 10: Variation of the COP with the adsorbate critical density

Despite the large errors of the present analysis, making equivalent the cases of COPs in the range 0.6-0.8, it still enables relative comparisons between materials. Fig. 11 offers a closer look in this range. Although the list of fluids in support material S2 is wide, it is not exhaustive and many of them can still be included in extended analyses. Fig. 11 shows many hazardous fluids and this discourages their application, especially for adsorption chillers, regarded as safe and environment friendly devices. Water, methanol, ammonia and ethanol are confirmed as being among the best fluids for adsorption cooling, although there are promising fluids which have been to date neglected such as 2-propanol.
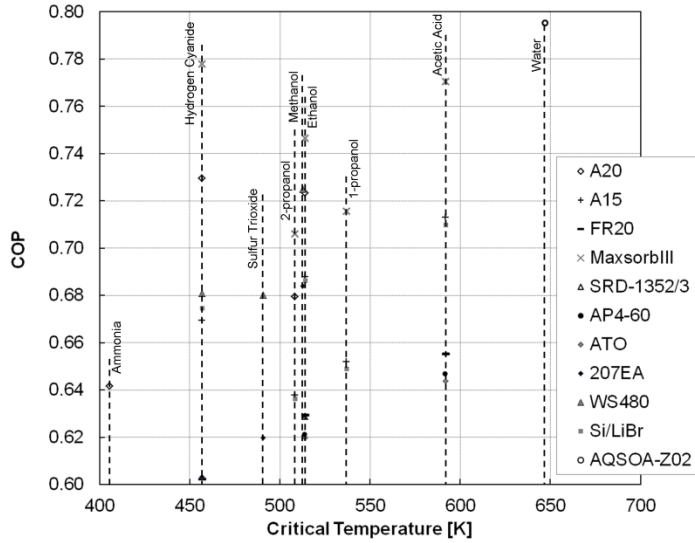

Figure 11: Variation of the COP with the adsorbate critical temperature in the range of COP from 0.6 to 0.8

11. Optimal fluid requirements for maximal COP

In order to univocally identify common leverage effects of the corresponding states parameters on the COP, the following set of quantities is calculated:

$$\frac{\partial COP}{\partial T_{cr}}\Delta T_{cr}; \ \frac{\partial COP}{\partial P_{cr}}\Delta P_{cr}; \ \frac{\partial COP}{\partial \rho_{cr}}\Delta \rho_{cr}; \ \frac{\partial COP}{\partial \omega}\Delta \omega; \ \frac{\partial COP}{\partial c_{p0,cr}}\Delta c_{p0,cr} \tag{22}$$

The values of $(\Delta T_{cr}, \Delta P_{cr}, \Delta \rho_{cr}, \Delta \omega, \Delta c_{p0,cr})$ are calculated as a ±30% neighbourhood of the critical values of the reference fluid. Acentric factor ω is correlated with P_{cr} by definition:

$$\omega = -log_{10}\left(\frac{P_{sat}}{P_{cr}}\right) - 1 \qquad \text{at } \frac{T_{sat}}{T_{cr}} = 0.7 \tag{23}$$

10

So, this correlation hinders the results of the sensitivity analysis on P_{cr}. Acentric factor has been intentionally conserved in this analysis since it is calculated by precise saturation pressure correlations. In our case, eq. (10) does not have the precision to allow substitution of ω with his definition. Results of the analysis on derivatives are reported in Fig. 12 for the three classes of adsorption materials investigated. Fig. 12 clarify on the sensitivity of COP to the change of fluid properties.

For all the working pairs, a decrease in the $c_{p0,cr}$ is beneficial for COP maximization. The effect of a change in $c_{p0,cr}$ is comparable in magnitude to those on ρ_{cr} and ω. Fluids with higher ρ_{cr} and ω enable higher COPs, although the magnitude depends on the specific material and on the reference fluid where the derivative is calculated. In all the cases, except MaxsorbIII/methanol and WS480/methanol, T_{cr} is the most important variable, affecting more than all the other variables the value of COP. The COP that one specific material can perform will result maximal if high T_{cr} fluids are used. This does not mean that all material will have high COP by using high T_{cr} fluids, rather high T_{cr} fluids enable the highest COPs that a material can achieve.

All the leverage effects already observed in the previous analysis are conserved across the materials, confirming the reliability of the analysis, although the magnitude of the effects depends on the specific material and on the reference fluid where the derivative is calculated.

Error bars in Fig. 12 quantify the standard deviation of each single variable in the investigated neighbourhood. This information is reported to assess the conservation of the derivatives throughout the neighbourhood. For all variables, the variance is lower than the central value, therefore the leverage effect on COP can change in the magnitude but not in the direction across the whole neighbourhood, meaning that fluids with high T_{cr}, ρ_{cr} and ω and with low $c_{p0,cr}$ favour higher COP.

Fig. 12 sheds light on the reason of the good performance that can be reached using water as refrigerant fluid, having water an extremely high T_{cr} and ρ_{cr}.

Other fluids such as ammonia, methanol and ethanol have T_{cr} well below water, but the combination of the other properties (ρ_{cr} and ω) make the final COP competitive to water (Table 4).

Accordingly, for an hypothetical material capable of adsorption of all fluids, methanol and ethanol will always show COPs lower than water and likely comparable with ammonia. Methanol will always provide COP higher than ethanol thanks to its higher ρ_{cr}. These conclusions are correct for the specific material as long as the leverage effect on COP is $T_{cr} > \rho_{cr} > \omega$, but this is not always the case as shown in Fig. 12.

Table 4: Thermodynamic properties of feasible fluids for adsorption cooling and heating

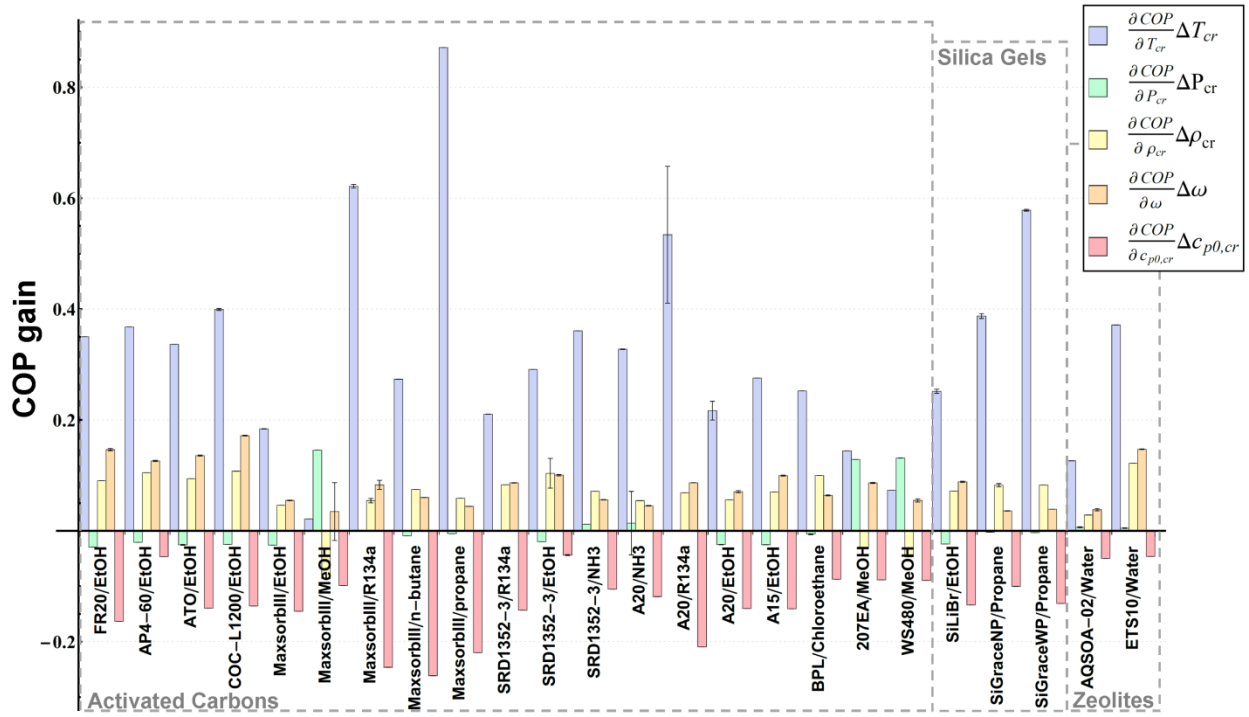|	Mol wt. [g mol^{-1}]	T_{cr} [K]	P_{cr} [kPa]	ρ_{cr} [mol m^{-3}]	Z_{cr}	ω	$C_{p0,cr}$ [kJ mol^{-1} K^{-1}]
methanol	32.042	512.64	8140	8547	0.224	0.566	0.061
ethanol	46.069	513.92	6120	5952	0.240	0.643	0.098
ammonia	17.031	405.65	11300	13889	0.241	0.253	0.038
water	18.015	647.30	22048	17857	0.228	0.344	0.037
1-propanol	60.096	536.78	5120	4545	0.252	0.617	0.135
2-propanol	60.096	508.30	4790	4525	0.250	0.670	0.133

Figure 12: Gain in the COP on change of fluid properties

12.Conclusion

An analysis on the sensitivity of COP on refrigerant fluid properties for adsorption heating and cooling has been performed by coupling the corresponding states principle with the characteristic curve of adsorption theory. The analysis has included 258 refrigerant fluids (support material S2) and 16 adsorption materials (Table 2). For the majority of materials, the fluid properties can have formidable leverage effect on COP. Adsorption heating or cooling is favoured by fluids having high critical temperature, whilst critical density and acentric factor are the second most important properties to enable the highest COP achievable to a material. For the majority of cases, leverage effect of the thermodynamic property of the fluid on COP was as follow: critical temperature > critical density > acentric factor. The present analysis highlights the need for synthesis of fluids tailored for adsorptive cooling application, which can significantly increase the COP exceeding the values achieved so far.

Acknowledgements

Nomenclature

COP	Coefficient of performance
$c_{p,refr}$	Refrigerant fluid isobaric specific heat capacity [kJ kg^{-1} K^{-1}]
$c_{p0,cr}$	Refrigerant fluid molar ideal gas specific heat capacity at critical temperature [kJ kg^{-1} K^{-1}]
$c_{p,ads}$	Refrigerant fluid isobaric specific heat capacity at a specific temperature [kJ kg^{-1} K^{-1}]
$\bar{c}_{p,ads}$	Average adsorbent specific heat capacity [kJ kg^{-1} K^{-1}] between maximal (T_{reg}) and minimal (T_{cond}) temperature of the thermodynamic cycle
$c_{p,refr}$	Refrigerant fluid isobaric specific heat capacity at specific thermodynamic conditions [kJ kg^{-1} K^{-1}]
$\bar{c}_{p,refr}$	Average refrigerant fluid molar specific heat capacity [kJ mol^{-1} K^{-1}] between two different states of the thermodynamic cycle

E	Characteristic energy for Dubinin-Astakhov isotherm [kJ mol^{-1}]	
K_{ref}	Dimensionless factor for the calculation of COP as defined in eq. (6)	
$K_{1,ads/ref}$	Dimensionless factor for the calculation of COP as defined in eq. (7)	
$K_{2,ads/ref}$	Dimensionless factor for the calculation of COP as defined in eq. (8)	
L	Refrigerant fluid molar latent heat [kJ mol^{-1}]	
P_{cr}	Refrigerant fluid critical pressure [kPa]	
P_{eq}	Equilibrium pressure [kPa]	
P_{sat}	Refrigerant fluid saturation pressure [kPa]	
q	Amount of moles adsorbed at specific (T, P) [mol kg^{-1}]	
q_{high}	Amount of mole adsorbed (high concentration) [mol kg^{-1}]	
q_{low}	Amount of mole adsorbed (low concentration) [mol kg^{-1}]	
q_s	Saturation adsorption capacity [mol kg^{-1}]	
Q_{des}	Desorption specific power [kJ kg^{-1}]	
Q_{ev}	Cooling specific power [kJ kg^{-1}]	
Q_{ph}	Isosteric heating specific power [kJ kg^{-1}]	
R	Universal gas constant [kJ mol^{-1} K^{-1}]	
t	Exponent in the Dubinin-Astakhov isotherm	
T	Temperature [K]	
T_{cond}	Condensing temperature [K]	
T_{cr}	Refrigerant fluid critical temperature [K]	
T_{eq}	Equilibrium temperature [K]	
T_{ev}	Evaporation temperature [K]	
$T_{int,h}$	Intermediate temperature at the end of the isosteric heating phase [K]	
T_{reg}	Regeneration maximal temperature [K]	
V_p	Pore volume [m^3]	

Greek symbols

Δh_{ads}	Differential enthalpy of adsorption [kJ mol^{-1}]
ΔH_{ads}	Enthalpy of adsorption [kJ kg^{-1}]
ω	Refrigerant fluid acentric factor
ρ_{cr}	Refrigerant fluid critical density [mol kg^{-1}]
ρ_{sat}	Refrigerant fluid saturated liquid molar density [mol kg^{-1}]
θ	Fractional pore filling (q/q$_s$)
$C(\theta)$	Characteristic curve of adsorption
ΔG_{imm}	Gibbs energy of immersion [kJ mol^{-1}]
Ω	Grand potential of adsorption [kJ mol^{-1}]

References

[1] R.E. Critoph. Refrigeration and Heat Pumping with Sorption Processes. *International Journal of Refrigeration* 35 (2012) 487–489

[2] Z. Tamainot-Telto, S.J. Metcalf, R.E. Critoph, Y. Zhong, R. Thorpe. Carbon-ammonia pairs for adsorption refrigeration applications: ice making, air conditioning and heat pumping. *International Journal of Refrigeration* 32 (2009) 1212-1229.

[3] A. Freni, G. Maggio, A. Sapienza, A. Frazzica, G. Restuccia, S. Vasta. Comparative analysis of promising adsorbent/adsorbate pairs for adsorptive heat pumping, air conditioning and refrigeration. *Applied Thermal Engineering* 104 (2016) 85-95.

[4] F. Meunier. Adsorption heat powered heat pumps. *Applied Thermal Engineering* 61 (2013) 830-836.

[5] J.A.A. Gibson, A.V. Gromov, S. Brandani, E.E.B. Campbell. The effect of pore structure on the CO2 adsorption efficiency of polyamine impregnated porous carbons. *Microporous and Mesoporous Materials* 208 (2015) 129-139.

[6] G. Santori, M. Luberti. Thermodynamics of thermally-driven adsorption compression. *Sustainable Materials and Technologies* 10 (2016) 1–9.

[7] F.Q. Zhu, L. Jiang, L.W. Wang, R.Z. Wang. Experimental investigation on a MnCl2-CaCl2-NH3 resorption system for heat and refrigeration cogeneration. *Applied Energy* 181 (2016) 29–37.

[8] L.G. Gordeeva, M.V. Solovyeva, Y.I. Aristov. NH2-MIL-125 as a promising material for adsorptive heat transformation and storage. *Energy* 100 (2016) 18-24

[9] A.D. Grekova, I.S. Girnik, V.V. Nikulin, M.M. Tokarev, L.G. Gordeeva, Yu.I. Aristov. New composite sorbents of water and methanol "salt in anodic alumina": Evaluation for adsorption heat transformation. *Energy* 106 (2016) 231-239.

[10] S. Kayal, S. Baichuan, B.B. Saha. Adsorption characteristics of AQSOA zeolites and water for adsorption chillers. *International Journal of Heat and Mass Transfer* 92 (2016) 1120–1127.

[11] I.S. Girnik, Yu.I. Aristov. Dynamics of water vapour adsorption by a monolayer of loose AQSOA™-FAM-Z02 grains: Indication of inseparably coupled heat and mass transfer. *Energy* 114 (2016) 767-773.

[12] Y. Zhong, R.E. Critoph, R.N. Thorpe, Z. Tamainot-Telto. Dynamics of BaCl2-NH3 adsorption pair. *Applied Thermal Engineering* 29 (2009) 1180-1186.

[13] B. Dawoud, Y. Aristov. Experimental study on the kinetics of water vapor sorption on selective water sorbents, silica gel and alumina under typical operating conditions of sorption heat pumps. *International Journal of Heat and Mass Transfer* 46 (2003) 273-281.

[14] K. Habib, B. Choudhury, P.K. Chatterjee, B.B. Saha. Study on a solar heat driven dual-mode adsorption chiller. Energy 63 (2013) 133-141.

[15] H.T. Chua, K.C. Ng, A. Malek, T. Kashiwagi, A. Akisawa, B.B. Saha. Multi-bed regenerative adsorption chiller—improving the utilization of waste heat and reducing the chilled water outlet temperature fluctuation. *International Journal of Refrigeration* 24 (2001) 124–136.

[16] B.B. Saha, S. Koyama, T. Kashiwagi, A. Akisawa, K.C. Ng, H.T. Chua. Waste heat driven dual-mode, multi-stage, multi-bed regenerative adsorption system. *International Journal of Refrigeration* 26 (2003) 749–757.

[17] S.Z. Xu, L.W. Wang, R.Z. Wang. Thermodynamic analysis of single-stage and multi-stage adsorption refrigeration cycles with activated carbon-ammonia working pair. *Energy Conversion and Management* 117 (2016) 31-42.

[18] G Santori, A. Sapienza, A. Freni. A dynamic multi-level model for adsorptive solar cooling. *Renewable Energy* 43 (2012) 301-312.

[19] S. Santamaria, A. Sapienza, A. Frazzica, A. Freni, I.S. Girnik, Yu. I. Aristov. Water adsorption dynamics on representative pieces of real adsorbers for adsorptive chillers. *Applied energy* 134 (2014) 11-19.

[20] A. Freni, L. Bonaccorsi, L. Calabrese, A. Caprì, A. Frazzica, A. Sapienza. SAPO-34 coated adsorbent heat exchanger for adsorption chillers. *Applied thermal engineering* 82 (2015) 1-7.

[21] R. E. Critoph. Performance Limitations of adsorption cycles for solar cooling. *Solar Energy* 41 (1988) 21-31.

[22] Yu.I. Aristov. Concept of adsorbent optimal for adsorptive cooling/heating. *Applied Thermal Engineering* 72 (2014) 166-175.

[23] Y Teng, R.Z Wang, J.Y Wu. Study of the fundamentals of adsorption systems. *Applied Thermal Engineering* 17 (1997) 327-338.

[24] M. Pons, F. Meunier, G. Cacciola, R.E. Critoph, M. Groll, L. Puigjaner, B. Spinner, F. Ziegler. Thermodynamic based comparison of sorption systems for cooling and heat pumping. *International Journal of Refrigeration* 22 (1999) 5–17.

[25] Yu.I. Aristov. Adsorptive transformation of heat: principles of construction of adsorbents database. *Applied Thermal Engineering* 42 (2012) 18-24.

[26] Prof. Orhan Talu letter to the members of the International Adsorption Society. http://ias.vub.ac.be/Database.html

[27] A. M. Tolmachev, I. A. Godovikov, T. A. Kuznetsova, and N. G. Kryuchenkova. A Computer Adsorption Database. *Protection of Metals and Physical Chemistry of Surfaces* 52 (2016) 372–375.

[28] NIST/ARPA-E Database of Novel and Emerging Adsorbent Materials. http://adsorbents.nist.gov/

[29] Springer Materials Adsorption Database

[30] D. Valenzuela, A.L. Myers. Adsorption Equilibrium Data Handbook (Prentice Hall advanced reference series)

[31] B.E. Poling, J.M. Prausnitz, J.P. O'Connell. Properties of Gases and Liquids, Fifth Edition, 2001 McGraw-Hill Education.

[32] S. Sircar, A.L. Myers. Characteristic adsorption isotherm for adsorption of vapors on heterogeneous adsorbents. *AIChE Journal* 32 (1986) 650–656.

[33] A. Freni, B. Dawoud, L. Bonaccorsi, S. Chmielewski, A. Frazzica, L. Calabrese, G. Restuccia. Characterization of Zeolite-Based Coatings for Adsorption Heat Pumps. SPRINGER BRIEFS IN APPLIED SCIENCES AND TECHNOLOGY. 2015 ISBN 978-3-319-09326-0 ISSN 2191-530X. Springer Cham Heidelberg New York Dordrecht London

[34] G. Soave. Equilibrium constants from a modified Redlich-Kwong equation of state. Chemical Engineering Science 27 (1972) 1197–1203.

[35] D.Y. Peng, D. B. Robinson. A New Two-Constant Equation of State. Industrial and Engineering Chemistry Fundamentals 15 (1976) 59-64.

[36] C.E. Bertrand, J.L. Self, J.R.D. Copley, A. Faraone. Dynamic signature of molecular association in methanol. *The Journal of Chemical Physics* 145 (2016) 014502.

[37] A. Grenner, G.M. Kontogeorgis, M.L. Michelsen, G.K. Folas. On the estimation of water pure compound parameters in association theories. *Molecular Physics* 105 (2007) 1797-1801.

[38] S. Velasco, M.J. Santos, J.A. White. Extended corresponding states expressions for the changes in enthalpy, compressibility factor and constant-volume heat capacity at vaporization. *Journal of Chemical Engineering Thermodynamics* 85 (2015) 68-76.

[39] A. Mulero, I. Cachadina, M.I. Parra. Liquid saturation density from predictive correlations based on the corresponding states principle: Part 1: Results for 30 families. *Industrial and Engineering Chemistry Research* 45 (2006) 1840-1848.

[40] H.W. Xiang, U.K. Deiters. A new generalized corresponding-states equation of state for the extension of the Lee–Kesler equation to fluids consisting of polar and larger nonpolar molecules. *Chemical Engineering Science* 63 (2008) 1490–1496

[41] Mark O. McLinden, Optimum refrigerants for non-ideal cycles: an analysis employing corresponding states. (1990) International Refrigeration and Air Conditioning Conference. Paper 89. http://docs.lib.purdue.edu/iracc/89

[42] B.L. Lee, M.G. Kesler. A generalized thermodynamic correlation based on three-parameter corresponding states. *AIChE Journal* 21 (1975) 510–527.

[43] Dortmund Data Bank: http://www.ddbst.com/

[44] M. Murialdo, N.P. Stadie, C.C. Ahn, B. Fultz. A Generalized Law of Corresponding States for the Physisorption of Classical Gases with Cooperative Adsorbate–Adsorbate Interactions. *Journal of Physical Chemistry C* 120 (2016) 11847–11853.

[45] D. F. Quinn. Supercritical Adsorption of 'Permanent' Gases under Corresponding States on Various Carbons. *Carbon* 40 (2002) 2767–2773.

[46] S. Sircar, S. Pramanik, J. Li, M.W. Cole, A.D. Lueking. Corresponding States Interpretation of Adsorption in Gate-Opening Metal-Organic Framework Cu(dhbc)(2)(4,4'-bpy). Journal of Colloid and Interface Science 446 (2015) 177–184.

[47] L.G. Gurvitsch. J. Russ. Phys. Chem. Soc. 47 (1915) 805-812

[48] W. Bachmann. Über einige Bestimmungen des Hohlraumvolumens im Gel der Kieselsäure. Zeitschrift für anorganische und allgemeine Chemie. 79 (1912) 202-208

[49] J.S. Anderson. Structure of silicic acid gels. Z. Physik. Chem. 88 (1914) 191-228

[50] L. Sliwinska, B.H. Davis. The Gurvitsch rule: an example of a rule misnamed? Ambix 34 (1987) 81-88

[51] T. Horikawa, D.D. Do, D. Nicholson. Capillary condensation of adsorbates in porous materials. *Advances in Colloid and Interface Science* 169 (2011) 40–58.

[52] A. A. Shapiro, E.H. Stenby. Analysis of Multicomponent Adsorption Close to a Dew Point. *Journal of Colloid and Interface Science* 206 (1998) 546-557.

[53] S.P. Tan, M. Piri. Equation-of-state modeling of confined-fluid phase equilibria in nanopores. *Fluid Phase Equilibria* 393 (2015) 48–63.

[54] D.D. Do. Adsorption Analysis: Equilibria and Kinetics, Vol. 2. World Scientific, 1998

[55] Z. Tamainot-Telto, S.J. Metcalf, R.E. Critoph, Y. Zhong, R. Thorpe. Carbon-ammonia pairs for adsorption refrigeration applications: ice making, air conditioning and heat pumping. *International Journal of Refrigeration* 32 (2009) 1212-1229.

[56] B.B. Saha, I.I. El-Sharkawy, R. Thorpe, R.E. Critoph. Accurate adsorption isotherms of R134a onto activated carbons for cooling and freezing applications. *International Journal of Refrigeration* 35 (2012) 499–505.

[57] I.I. El-Sharkawy, K. Kuwahara, B.B. Saha, S. Koyama, K.C. Ng. Experimental investigation of activated carbon fibers/ethanol pairs for adsorption cooling system application. *Applied Thermal Engineering* 26 (2006) 859-865.

[58] W.S. Loh, A.B. Ismail, B. Xi, K.C. Ng, W.G. Chun. Adsorption Isotherms and Isosteric Enthalpy of Adsorption for Assorted Refrigerants on Activated Carbons. *Journal of Chemical and Engineering Data* 57 (2012) 2766-2773.

[59] V. Brancato, A. Frazzica, A. Sapienza, L. Gordeeva, A. Freni. Ethanol adsorption onto carbonaceous and composite adsorbents for adsorptive cooling system. *Energy* 84 (2015) 177-185

[60] I.I. El-Sharkawy, B.B. Saha, S. Koyama, J. He, K.C. Ng, C. Yap. Experimental investigation on activated carbon–ethanol pair for solar powered adsorption cooling applications. *International Journal of Refrigeration* 31 (2008) 1407-1413.

[61] I.I. El-Sharkawy, M. Hassan, B.B. Saha, S. Koyama, M.M. Nasr. Study on adsorption of methanol onto carbon based adsorbents. *International Journal of Refrigeration* 35 (2009) 1579-1586.

[62] B.B. Saha, K. Habib, I.I. El-Sharkawy, S. Koyama. Adsorption characteristics and heat of adsorption measurements of R-134a on activated carbon. *International Journal of Refrigeration* 32 (2009) 1563-1569.

[63] S. Saha, A. Chakraborty, B.B. Saha, S. Koyama. Performance study of adsorption characteristics of silica gel-water, activated carbon-n-butane systems. Proceedings of the 4th BSME-ASME International Conference on Thermal Engineering, Paper No. 149, Dhaka, pp. 159-164, December 27-29, 2008.

[64] B.B. Saha, I.I. El-Sharkawy, R. Thorpe, R.E. Critoph. Accurate adsorption isotherms of R134a onto activated carbons for cooling and freezing applications. *International Journal of Refrigeration* 35 (2012) 499-505.

[65] Y. Wang, M.D. LeVan. Nanopore Diffusion Rates for Adsorption Determined by Pressure-Swing and Concentration-Swing Frequency Response and Comparison with Darken's Equation. *Industrial and Engineering Chemistry Research* 47 (2008) 3121-3128.

[66] J.W. Wu, S.H. Madani, M.J. Biggs, P. Phillip, C. Lei, E.J. Hu. Characterizations of Activated Carbon–Methanol Adsorption Pair Including the Heat of Adsorptions. *Journal of Chemical and Engineering Data* 60 (2015) 1727-1731.

[67] C.A. Grande, A.E. Rodrigues. Adsorption Equilibria and Kinetics of Propane and Propylene in Silica Gel. *Industrial and Engineering Chemistry Research* 40 (2001) 1686-1693.

[68] S. Kayal, S. Baichuan, B.B. Saha. Adsorption characteristics of AQSOA zeolites and water for adsorption chillers. *International Journal of Heat and Mass Transfer* 92 (2016) 1120-1127.

[69] G. Santori, A. Frazzica, A. Freni, M. Galieni, L. Bonaccorsi, F. Polonara, G. Restuccia. Optimization and testing on an adsorption dishwasher. *Energy* 50 (2013) 170-176.

[70] J.M. Pinheiro, A.A. Valente, S. Salústio, N. Ferreira, J. Rocha, C.M. Silva. Application of the novel ETS-10/water pair in cyclic adsorption heating processes: Measurement of equilibrium and kinetics properties and simulation studies. *Applied Thermal Engineering* 87 (2015) 412-423.

[71] A.L. Myers. Thermodynamics of adsorption in porous materials. AIChE Journal 48 (2002) 145-160.